Higher-band modulational instability in photonic lattices

Christian E. Rüter, Jürgen Wisniewski, Milutin Stepić, and Detlef Kip

Institute of Physics and Physical Technologies, Clausthal University of Technology, Clausthal-Zellerfeld, Germany
d.kip@pe.tu-clausthal.de

Abstract: Propagation of extended Floquet-Bloch modes in the first three bands of a one-dimensional photonic lattice possessing a self-defocusing saturable nonlinearity is studied experimentally and numerically on the example of waveguide arrays in lithium niobate. Discrete modulation instability is observed in all bands in the region of anomalous diffraction, whereas modes propagate stable in the normal diffraction regime.

OCIS codes: (230.7330) Waveguides; (190.4420) Nonlinear optics, transverse effect in; (190.5530) Pulse propagation and solitons.

References and links

1. A. Hasegawa, "Theory and computer experiment on self-trapping instability of plasma cyclotron," Phys. Fluids **15**, 870 (1972).
2. T. B. Benjamin and J. E. Feir, "Disintegration of wave trains on deep water," J. Fluid Mech. **27**, 417 (1967).
3. P. Marquie, J. M. Bilbaut, and M. Remoissenet, "Generation of envelope and hole solitons in an experimental transmission line," Phys. Rev. E **49**, 828 (1994).
4. K. E. Strecker, G. B. Partridge, A. G. Truscott, and R. G. Hulet, "Formation and propagation of matter-wave soliton trains," Nature **417**, 150 (2002).
5. K. Tai, A. Hasegawa, and A. Tomita, "Observation of modulational instability in optical fibers," Phys. Rev. Lett. **56**, 135 (1986).
6. M. I. Carvalho, S. R. Singh, and D. N. Christodoulides, "Modulational instability of quasi-plane-wave optical beams biased in photorefractive crystals," Opt. Commun. **126**, 167 (1996).
7. D. Kip, M. Soljačić, M. Segev, E. Eugenieva, and D. N. Christodoulides, "Modulation instability and pattern formation in spatially incoherent light beams," Science **290**, 495 (2000).
8. D. N. Christodoulides, F. Lederer, and Y. Silberberg, "Discretizing light behavior in linear and nonlinear waveguide lattices," Nature **424**, 817 (2003).
9. Yu. S. Kivshar and M. Peyrard, "Modulation instabilities in discrete lattices," Phys. Rev. A **46**, 3198 (1992).
10. D. N. Christodoulides and R. I. Joseph, "Discrete self-focusing in nonlinear arrays of coupled waveguides," Opt. Lett. **19**, 794 (1988).
11. H. S. Eisenberg, Y. Silberberg, R. Morandotti, A. R. Boyd, and J. S. Aitchison, "Discrete spatial optical solitons in waveguide arrays," Phys. Rev. Lett. **81**, 3383 (1998).
12. F. Chen, M. Stepić, C. E. Rüter, D. Runde, D. Kip, V. Shandarov, O. Manela, and M. Segev, "Discrete diffraction and spatial gap solitons in photovoltaic $LiNbO_3$ waveguide arrays," Opt. Express **13**, 4314 (2005).
13. D. Mandelik, H. S. Eisenberg, Y. Silberberg, R. Morandotti, and J. S. Aitchison, "Band-gap structure of waveguide arrays and excitation of Floquet-Bloch solitons," Phys. Rev. Lett. **90**, 053902 (2003).
14. J. Meier, G. I. Stegeman, D. N. Christodoulides, Y. Silberberg, R. Morandotti, H. Yang, G. Salamo, M. Sorel, J. S. Aitchison, "Observation of discrete modulational instability," Phys. Rev. Lett. **92**, 163902 (2004).
15. M. Stepić, C. Wirth, C. E. Rüter, and D. Kip, "Observation of modulation instability in discrete media with self-defocusing nonlinearity," Opt. Lett. **31**, 247 (2006).
16. C. E. Rüter, J. Wisniewski, and D. Kip, "Prism coupling method to excite and analyze Floquet-Bloch modes in linear and nonlinear waveguide arrays," Opt. Lett. **31**, 2768 (2006).
17. J. Vollmer, J. P. Nisius, P. Hertel, and E. Krätzig, "Refractive index profiles of $LiNbO_3$:Ti waveguides," Appl. Phys. A **32**, 125 (1983).
18. M. Stepić, C. E. Rüter, D. Kip, A. Maluckov, and Lj. Hadžievski, "Modulational instability in one-dimensional saturable waveguide arrays: comparison with Kerr nonlinearity," Opt. Commun. **267**, 229 (2006).

1. Introduction

Modulational instability (MI) is a universal phenomenon common to many nonlinear wave systems. Due to the interplay between nonlinearity and dispersion a propagating plane wave can become unstable to amplitude or phase modulations of certain frequencies which grow exponentially. Such filamentation of extended plane waves can result in a train of localized

#81410 - $15.00 USD Received 23 Mar 2007; revised 2 May 2007; accepted 2 May 2007; published 7 May 2007

intensity, which can be regarded as an ensemble of separated solitons. MI has been investigated in various physical systems, for example plasmas [1], fluids [2], electrical circuits [3], Bose Einstein condensates [4], optical fibers [5], and crystals [6,7], to mention a few.

In periodic systems, the extended states are Floquet-Bloch (FB) modes, and nonlinearity may also cause MI [8, 9]. In the optics case, the linear FB modes form a transmission spectrum consisting of allowed bands, separated by gaps where light propagation is forbidden. In each band discrete diffraction can be either normal or anomalous; in a limited region nearly diffraction-free propagation becomes possible, too [8]. For nonlinear optical lattices the sign of diffraction has a large impact on the stability of propagating modes [9]: Modes exhibiting normal diffraction undergo MI in the presence of self-focusing, whereas modes displaying anomalous diffraction break up under self-defocusing, forming ensembles of discrete solitons [10-13]. The first case has been shown in one-dimensional (1D) lattices with self-focusing Kerr nonlinearity in Al GaAs [13,14], whereas the latter defocusing system has been realized in a 1D lattice fabricated in lithium niobate ($LiNbO_3$) [15]. However, in both cases investigations were limited to light propagating in the 1st band of the photonic lattice. In this contribution we explore MI in higher bands of a 1D nonlinear waveguide array (WA) in $LiNbO_3$, a material that possesses a saturable defocusing nonlinearity. The consequences arising from the saturable nature of the nonlinearity on the stability of the formed filaments is investigated within the 1st band, and the influence of the coupling strength of adjacent channels on the spatial frequency of the filaments is presented for MI in the 2nd and 3rd band.

2. Experimental methods

Permanent WA with channels close enough to allow for tunneling of energy from one waveguide to its neighbours were prepared using *x*-cut $LiNbO_3$ with sample sizes of 1mm × 22mm × 7.8 mm along the crystallographic *x*, *y* and *z*-axis [12]. The channels are directed parallel to the *y*-axis, while the *z*-axis coincides with the ferroelectric *c*-axis. First an 8.6 nm thick iron layer was in-diffused for 22 h at 1273 K to increase the photorefractive effect. Next, an evaporated 5 nm thick Ti layer was patterned using standard lithographic techniques. Two different arrays with grating periods Λ = 8 μm and Λ = 9 μm, respectively, were fabricated, each consisting of 250 stripes with a fixed width of 5 μm. Before annealing for 2 hours at 1273 K a second planar Ti layer with a thickness of 5 nm has been deposited on the patterned surface. The resulting refractive index profile is a superposition of a WA and a planar waveguide. Finally, the end facets of the samples were polished to optical quality.

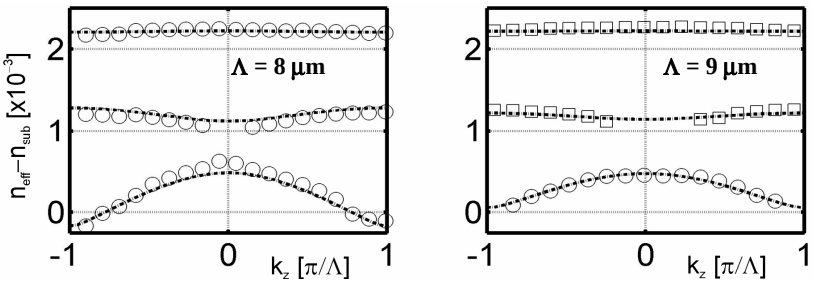

Fig. 1. Measured (symbols) and calculated (lines) band structure of the two arrays used with grating periods 8 μm [left hand side (lhs)] and 9 μm [right hand side (rhs)].

For the excitation of pure FB modes as well as for the measurement of band structures of our samples we used a prism coupling setup and extraordinary polarized coherent green light with wavelength λ = 514 nm [16]. The size of the coupling area was adjusted to comprise all 250 channels of the arrays. The propagation length was set to be 15 mm in all experiments and a CCD camera was used to monitor the rear facet of the WA. Figure 1 shows the effective refractive index increase $n_{eff} = \beta/k_0$ of the excited FB modes as a function of transverse wave vector k_z. Here n_{sub} is the $LiNbO_3$ substrate refractive index and $k_0 = 2\pi/\lambda$. For both samples the band structures show three guided bands (i.e., $n_{eff} - n_{sub} > 0$). An increase of the distance

#81410 - $15.00 USD Received 23 Mar 2007; revised 2 May 2007; accepted 2 May 2007; published 7 May 2007

between waveguides corresponds to a decrease of diffraction (weaker evanescent coupling of adjacent channels). This effect can be seen best for the 3rd band, where diffraction for the sample with Λ = 9 μm is weaker than diffraction for the sample with Λ = 8 μm while the band-gap between 2nd and 3rd band has spread.

3. Numerical modeling of wave propagation

We perform numerical simulations based on a (1+1) D beam propagation method to support our experiments. First, to obtain the effectively 1D index profile, the diffusion equation is solved for the patterned Ti stripes. From the resulting Ti concentration the index profile is derived using [17] and the spatial index distribution at the surface is extracted. The amplitude of the refractive index modulation $n(z)$ is afterwards adjusted to fit the experimental results. $LiNbO_3$ exhibits a non-instantaneous, defocusing saturable nonlinearity that is due to the photorefractive effect [12]. The nonlinearity is described by $\Delta n = -\Delta n_{sat}[I/(I+I_d)][1-\exp(-t/\tau)]$ with intensity I, dark irradiance I_d, saturation value Δn_{sat} and an intensity dependent time constant $\tau \sim 1/(I+I_d)$. To simulate the time dependent output intensity distribution for excitation of FB modes the following procedure is implemented. First, white noise is added to the field distribution of the investigated FB mode and the propagation of this mode is calculated. The nonlinear index changes $\Delta n(z)$ induced by the corresponding intensity distribution $I(z)$ during time interval Δt are added to the initial (permanent) index modulation $n(z)$ and the propagation of the initial mode is calculated using the resulting refractive index distribution $n(z) + \Delta n(z)$. This procedure is repeated until the time steps Δt add up to the total time t_{end}. In all simulations the saturation value of the nonlinear refractive index change is set to $\Delta n_{sat} = 3.5 \times 10^{-4}$ and the time is normalized to the time constant τ_3 for a ratio $I/I_d = 3$. In the simulations a WA consisting of 250 channels is used. Related to the experimental procedure (see next paragraph) the intensity distribution after 15 mm of propagation is extracted from the simulations and plotted as a function of time. Furthermore, in the simulation results in the following section we provide the line profiles of intensity at $t = 0$ (lhs of plot) and $t = t_{end}$ (rhs of plot).

4. Experimental and numerical results

Because of the low scattering level of light in our samples only the intensity on the rear sample facet can be monitored using a CCD camera. Related to the slow response of the involved photorefractive nonlinearity, one image of the rear facet is taken every minute, resulting in the time dependent intensity evolutions monitored below. Additionally, each experimental figure contains the first ($t \approx 0$, lhs) and last ($t = t_{end}$, rhs) image displayed together with an intensity line plot. First, we investigate MI in the sample with lattice period Λ = 8 μm. To study the influence of the saturable nature of the nonlinearity on the formation of localized states during MI, the 1st band is excited at the edge of the BZ using different input powers P_{in} (defined as total incoupled power into ≈ 250 channels). In the experiments as well as in the simulations three different regions can be distinguished. For the low incoupled power in Figs. 2(a) and 2(d) a rather long build-up time of the instability is observed, while the contrast of the filamentation is generally weak. Consequently, the emerging localized states comprise several waveguides and overlap with each other. For medium input power in Figs. 2(b) and 2(e) the build-up time constant is reduced. At the same time the final intensity contrast is improved, connected with the formation of narrow localized states. As can be seen [Fig. 2(b)] the filaments comprise about 1–2 waveguides and are stable for times large compared to the build-up time constant. If the input power is increased further in Figs. 2(c) and 2(f), the build-up time is again decreased but now nonlinearity starts to saturate, resulting in broadening of the initially formed filaments with time, and finally a complete wash-out of the structures [7]. This proves that MI may be suppressed completely when saturation of the nonlinearity is strong [18].

#81410 - $15.00 USD Received 23 Mar 2007; revised 2 May 2007; accepted 2 May 2007; published 7 May 2007

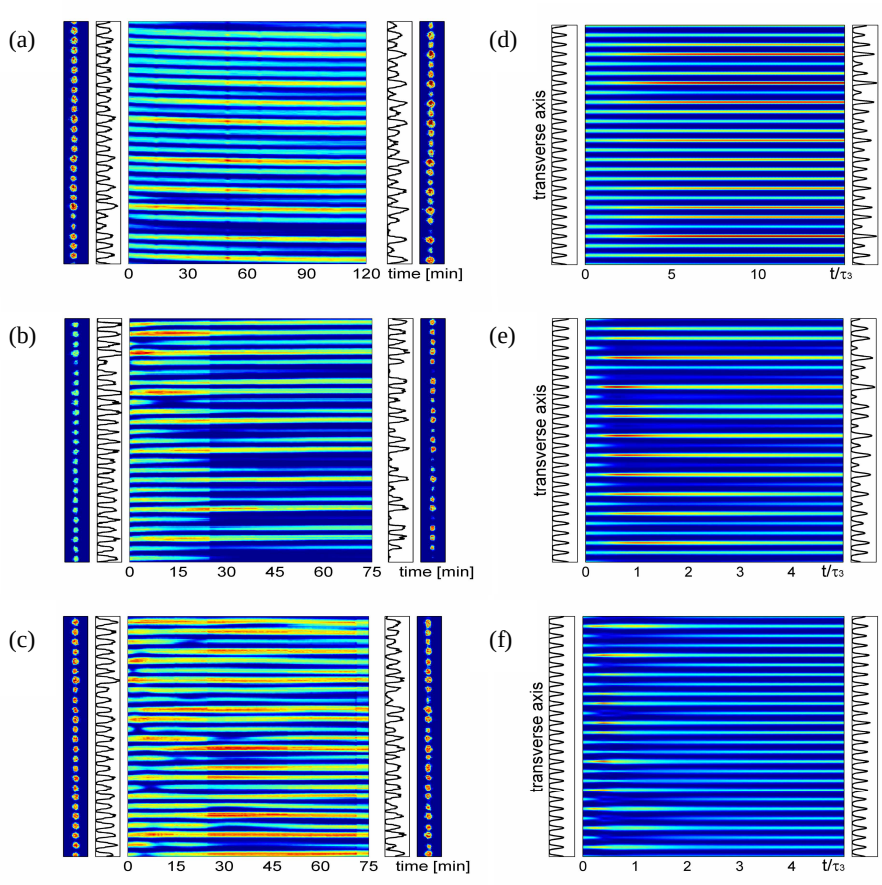

Fig. 2. Time dependent output intensity at the rear facet of a WA with period Λ = 8 µm in the 1st band at the edge of the BZ for input powers (a) 2 µW, (b) 10µW, and (c) 26 µW. Corresponding simulations with intensity ratios I/I_d = 0.5 (d), I/I_d = 3 (e), and I/I_d = 9 (f).

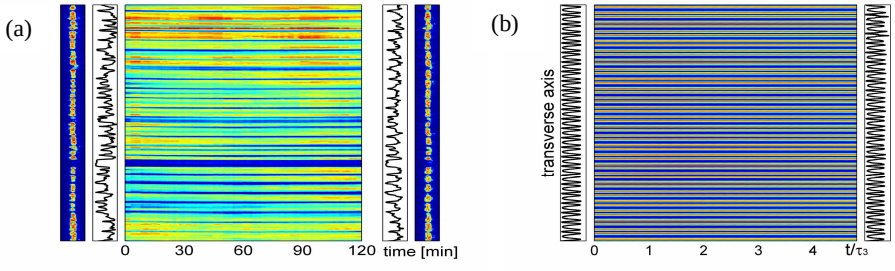

Fig. 3. (a). Absence of MI in 2nd band at $k_z = \pi/\Lambda$ for P_{in} = 6 µW. (b) Simulation with I/I_d = 1.

When moving to the 2nd band, in Fig. 3 we prove that MI is absent for normal diffraction at the edge of the BZ for any recording time [8]. On the other hand, MI is expected to occur in the anomalous diffraction regime around the center of the BZ. However, to generate such waves direct excitation with $k_z = 0\ \pi/\Lambda$ in the prism set-up [16] can hardly be used because of the vanishing overlap of the input plane wave with such a mode (see missing symbols for this situation in Fig. 1). Therefore a value of $2\pi/\Lambda$ is chosen for k_z corresponding to the center of the 2nd BZ and the corresponding results showing MI are given in Fig. 4. Compared to MI in the 1st band, here stronger coupling results in broader products of MI (lower spatial frequency) [18]. With increasing input power the contrast of the filaments is further increased.

#81410 - $15.00 USD Received 23 Mar 2007; revised 2 May 2007; accepted 2 May 2007; published 7 May 2007

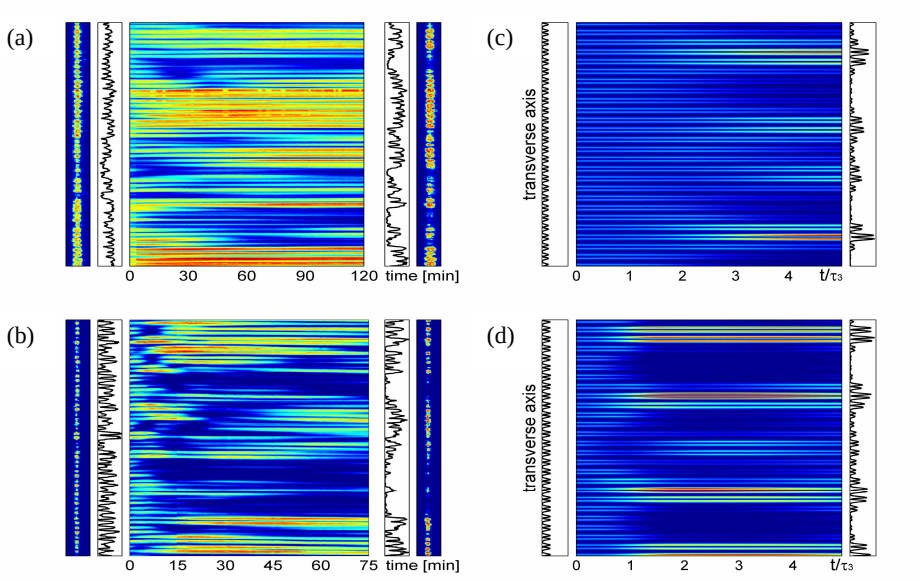

Fig. 4. Discrete MI in the 2nd band of a WA with $\Lambda = 8$ µm at $k_z = 2\pi/\Lambda$ for $P_{in} = 7$ µW (a) and $P_{in} = 21$ µW. (b) Simulations with $I/I_d = 1$ (c) and $I/I_d = 3$ (d).

In the 3rd band MI is expected to occur for modes excited at the edge of the BZ [8]. From the band structure measurements in Fig. 1 it can be seen that diffraction of these modes of the 3rd band is stronger when compared to the 2nd band (at $k_z = 0$). With the nonlinearity being limited to the saturation value Δn_{sat} for all bands, modes of the 3rd band are expected to disintegrate (for $k_z = \pi/\Lambda$) into larger filaments than modes of the 2nd band (for $k_z = 0$). From the simulation of this situation monitored in Fig. 5(b) filament sizes can be expected to be almost too big to be studied with the current setup, where observation of the rear facet is limited to about 25 channels. Nevertheless, in the experimental results in Fig. 5(a) a corresponding broad filamentation of the output light intensity may be observed, although the modulation is rather weak. Obviously, diffraction of this sample in the 3rd band is almost too strong with respect to the "available" nonlinearity. On the other hand, no signs of MI are observed for modes of the 3rd band at the center of the BZ ($k_z = 0$), in full agreement with theoretical predictions.

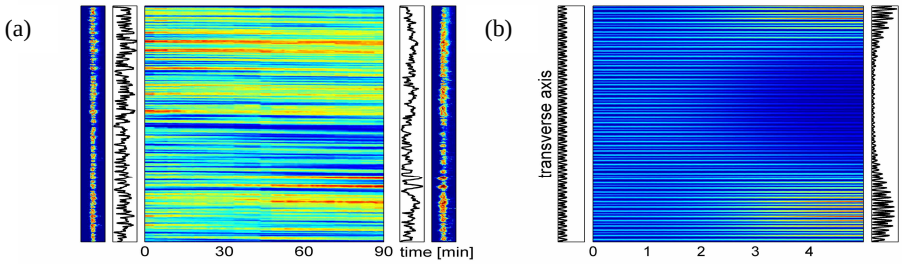

Fig. 5. (a). Discrete MI in the 3rd band of a WA with $\Lambda = 8$ µm at $k_z = \pi/\Lambda$ and $P_{in} = 20$ µW. (b) Corresponding simulation with $I/I_d = 1$.

To investigate the dependence of the spatial frequency of intensity modulations during MI on the diffraction properties of the lattices, the experiments were repeated using the 2nd array with $\Lambda = 9$ µm. This array possesses smaller diffraction coefficients (see "flatter" bands in Fig. 1) when compared to the one with $\Lambda = 8$ µm, thus smaller filament sizes are expected. This assumption is confirmed both experimentally and numerically for the 2nd and 3rd band in

#81410 - $15.00 USD Received 23 Mar 2007; revised 2 May 2007; accepted 2 May 2007; published 7 May 2007

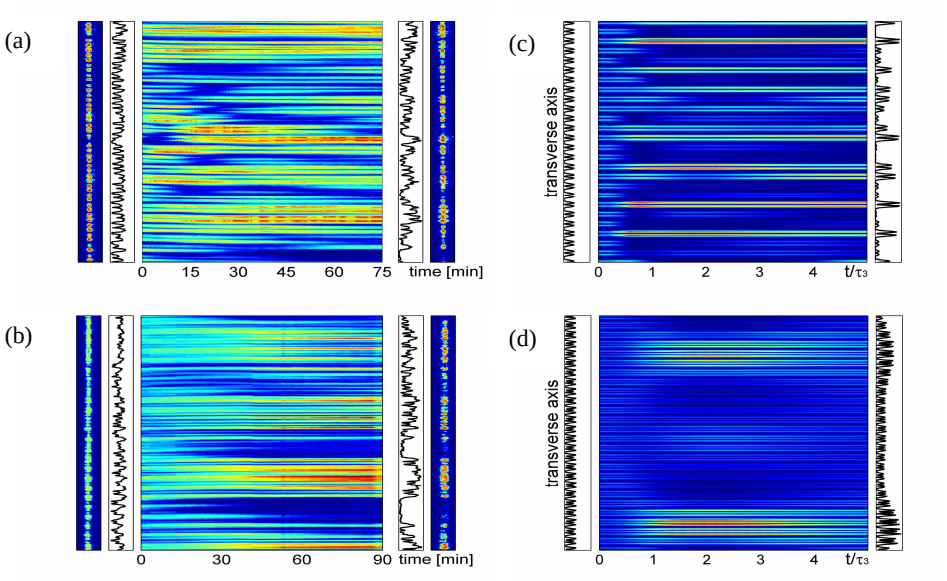

Fig. 7. Discrete MI in a WA with $\Lambda = 9$ µm: (a) 2nd band at $k_z = 2\pi/\Lambda$ and $P_{in} = 20$ µW. (b) 3rd band at $k_z = \pi/\Lambda$ and $P_{in} = 7$ µW. (c,d) Corresponding simulations with $I/I_d = 3$.

Fig. 6. In the 2nd band, narrow filaments comprising only 2–3 channels are observed, which is significantly smaller then those found in the array with $\Lambda = 8$ µm (see Fig. 4). Similarly, in the 3rd band filament sizes are reduced from about 10–12 channels for the lattice with $\Lambda = 8$ µm to 5–7 channels for the lattice with $\Lambda = 9$ µm.

5. Summary

In summary, discrete MI of FB modes within the first three bands of permanent 1D WA's with self-defocusing nonlinearity is reported. The spatial instabilities are observed only in the regime of anomalous diffraction. Furthermore, we demonstrate both experimentally and numerically that discrete MI does not develop in the regime of normal diffraction, in full agreement with theoretical predictions. In addition, the influence of the saturable nature of the nonlinearity on both existence and stability of the filaments is discussed for processes within the 1st band. The correlation between coupling strength and spatial frequency of patterns for fixed value of the maximum refractive index change is qualitatively confirmed, too.

Acknowledgment

This research was supported by the Deutsche Forschungsgemeinschaft (DFG grants Ki482/8-1 and Ki482/8-2).

#81410 - $15.00 USD Received 23 Mar 2007; revised 2 May 2007; accepted 2 May 2007; published 7 May 2007